PASSIVE A-BAND WIND SOUNDER (PAWS) FOR MEASURING TROPOSPHERIC WIND VELOCITY

Shane Roark, Robert Pierce, Christian Grund, Philip Slaymaker, Pei Huang, and Paul Kaptchen

Ball Aerospace & Technologies Corporation
1600 Commerce Street
Boulder, Colorado, 80306-1062

ABSTRACT

The Passive A-Band Wind Sounder (PAWS) project is funded through NASA's Instrument Incubator Program (IIP). The objective of PAWS is to demonstrate an instrument concept for measuring wind speed profiles in the troposphere using Doppler shifts in selected oxygen absorption lines. PAWS is a daytime-only approach, but has the potential to provide better wind data than is currently available with significantly lower cost, risk, and platform requirements than lidar. This paper will provide an overview of the PAWS approach and progress on the instrument development.

1. INTRODUCTION

Measurement of the global tropospheric wind profile is important for improving weather forecasting and understanding atmospheric transport and mixing of chemical and aerosol species. Weather balloons and radiosondes provide good local information about wind, but only probe a small fraction of the desired global coverage and do not retrieve any information about wind over the oceans. Satellite observations provide ocean and global coverage by monitoring the movement of clouds and waves to determine wind speed and direction. The limitation with these approaches is that they cannot measure wind as a function of altitude throughout the atmosphere. Computer models routinely are used to estimate global winds based on satellite data of other atmospheric parameters, such as temperature and humidity. Although these models generate very good wind approximations, direct global measurement of wind speed and direction as a function of altitude in the troposphere would provide new information and detail for understanding atmospheric dynamics, including the processes that affect climate, weather, natural hazards, and transportation of pollutants. According to the recent NRC Decadal Survey, tropospheric winds are the number one unmet measurement objective for improving weather forecasts [1].

The objective for PAWS is to demonstrate an instrument concept for measuring tropospheric wind speed profiles from Doppler shifts in oxygen absorption features. PAWS is a daytime-only approach and will not provide the level of accuracy, precision, or spatial resolution that is anticipated for Doppler lidar. However, PAWS does have the potential to provide much better wind data than is available in the near term with significantly lower cost, risk, and platform requirements than lidar. The PAWS instrument is small and lightweight, and the components have proven space heritage. Because the signal comes from scattered sunlight, PAWS does not require a powerful and reliable laser, high-speed detector or any high-power or high-voltage components, and is insensitive to altitude. The challenge for PAWS is not in development of the individual components, but rather to determine if the components can function collectively to provide the desired wind-profile data using absorption lines in the oxygen A-band.

2. OPERATION CONCEPT AND MEASUREMENT APPROACH

The baseline on-orbit operational concept for PAWS is summarized in **Fig. 1** and was derived from the Wind Imaging Interferometer (WINDII) on the Upper Atmosphere Research Satellite (UARS) [2]. From low-Earth orbit (LEO), the instrument views a one-dimensional atmospheric column from roughly the ground to 20 km in elevation. The atmospheric limb is resolved into individual elevation elements to obtain the line-of-site wind vectors as a function of altitude. The horizontal limb dimension will be set by the measurement integration time, which will be determined experimentally. For a baseline integration time of 30 seconds and a spacecraft ground speed of approximately 7 km/s, the width of the atmospheric column would be roughly 210 km. As shown in **Fig. 2**, the instrument will have fixed forward (FOV1) and rearward (FOV2) fields of view that are imaged simultaneously. The fields of view are oriented near 45° and 135° with respect to the spacecraft ground track to obtain the orthogonal horizontal wind vectors for each sampling volume. With this approach, there is a time lag of several minutes between the two spacecraft positions required to obtain the orthogonal wind vectors within the sample volume.

Since PAWS is a passive instrument, the spectral radiance along the entire line-of-sight is measured. Therefore, the data for a given altitude are contaminated by data from higher altitudes at other positions along the line-of-sight. There are two factors that reduce the significance of this complication. First, for a given

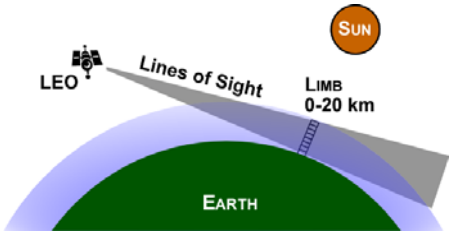

Fig. 1. Side view showing the on-orbit operation concept.

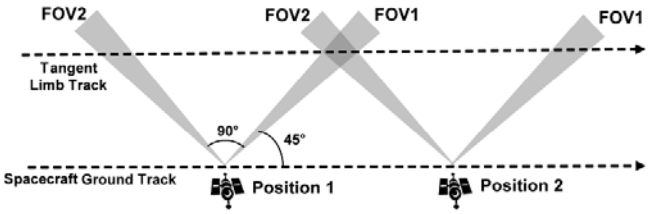

Fig. 2. Plan view showing the approach for measuring orthogonal wind vectors.

tangent line-of-sight, the optical path is relatively short through the higher altitude shells of the atmosphere and the density of oxygen decreases with altitude, so the contribution to the absorption spectrum is relatively small. Second, at the near and far ends of the tangent line where higher altitudes are inadvertently sampled, the line-of-sight is not horizontal with respect to the Earth surface, so the magnitude of the wind vector is reduced.

The oxygen A-band was selected for passive Doppler measurements because (1) the lines are not obscured by other features in the atmospheric absorption spectrum, (2) the lines are sharp and well-resolved, (3) a wide range of line absorption depths are available to optimize the signal-to-noise ratio (SNR), (4) the tracer molecule is abundant and uniformly distributed in the troposphere, and (5) the A-band is in a spectral region compatible with high-spectral-resolution technology and silicon detectors with high quantum efficiency.

The baseline filtering approach for PAWS is to isolate one or two absorption features in the A-band spectrum. The Doppler frequency shift, $\delta\nu$, in the absorption is expressed as a function of the component of wind velocity in the direction of the instrument, υ_w, according to [3],

$$\delta\nu = \nu_0 \frac{\upsilon_w}{c}, \qquad (1)$$

where ν_0 is the zero-wind absorption line center frequency and c is the speed of light. From this relationship, a 5 m/s wind speed would only shift the absorbance line center by about 10^{-4} cm^{-1}, which would not be resolvable by a grating spectrograph. However, when the filtered light is passed through a Michelson interferometer, the Doppler shift in the phase of the modulation of the interferogram, $\delta\phi$, is dependent on the optical path difference (OPD), τ, in the interferometer according to,

$$\delta\phi = 2\pi\nu_0\tau\frac{\upsilon_w}{c} + F(\tau), \qquad (2)$$

where $F(\tau)$ is a complicated function that depends upon the filtering method and the number of absorption lines being measured. Therefore, a large OPD can be used to accentuate the wind-induced frequency shift by measuring the phase shift of high-order fringes in the interferogram. The tradeoff is that the visibility of the interferogram decreases as the OPD increases, so a compromise must be reached to optimize the sensitivity of the measurement and the SNR.

3. INSTRUMENT DEVELOPMENT AND TESTING

During the first two years of this project, a breadboard instrument was designed, constructed, and tested. The breadboard was used as a path-finding tool and sacrificed stability in order to accommodate a number of possible orientations and measurement schemes. This approach enabled a thorough, yet economical assessment of the effect of each instrument component on the measurement. Test results demonstrated that all of the instrument components performed collectively to enable phase measurements with high resolution; however, instrument drift from thermal and mechanical instability precluded measurement of actual wind-induced Doppler shifts.

Results from breadboard testing, experimentation, and analysis were used to refine the engineering unit instrument design. Instrument stability is a critical design objective since the signal levels are small and measurements are accumulated for many seconds. Similarly, uniformity of the signal is critical since any variations in the optical irradiance will add noise. For practical purposes, aperture sharing is a requirement to reduce the number of components. **Fig. 3** shows a diagram of the engineering unit design. A single gimbaled telescope collects scattered light from a vertical column in its field-of-view. The gimbaled telescope is only for instrument development; the flight version would have fixed fore and aft fields-of-view as indicated in Fig. 2. Light is focused onto multimode optical fibers (represented at the bottom of the figure) that are positioned in a vertical array. The light in each fiber is homogenized with a high-speed scrambler prior to entering the filter section, which ensures that the filtering does not depend on modal variations. The filters aperture-share the set of light sources arrayed in cylindrical symmetry. A three-fold fiber array is shown in Fig. 3. After filtering, the fibers are again arrayed linearly for use in the interferometer. The interferogram from three

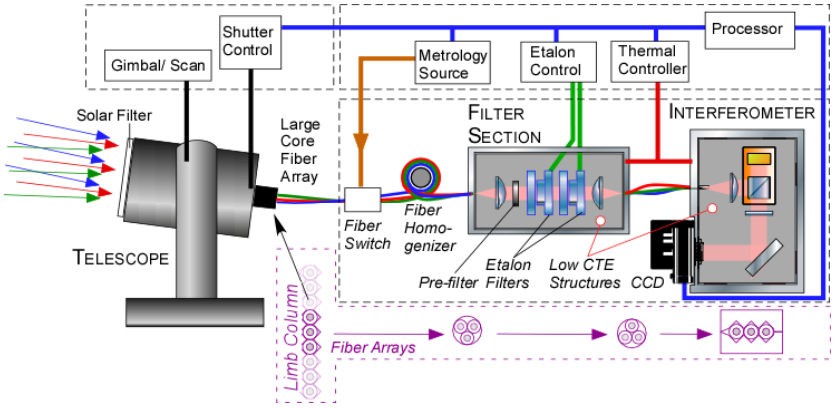

Fig. 3 Schematic view of the engineering unit for atmospheric measurements.

such sources is then line-focused on a single charge coupled device (CCD). The fiber is standard 62.5/125 graded index fiber (GIF) which allows for the use of several off-the-shelf components.

Although the instrument housings are constructed from low coefficient of thermal expansion (CTE) ceramic, thermal control on the order of 0.1 K over a measurement cycle is required for the filter and interferometer sections. A metrology source is used as a stable frequency reference, and the source can be either an RF-excited O_2 lamp or a tunable low power laser locked to the precise bottom of the appropriate O_2 absorption line. The reference is used as a frequency standard for tuning the filter(s), and for generating a reference interferogram. In the design shown in Fig. 3, an integrated signal from the CCD is used in a feedback loop to optimize the filter positions, but alternatives, such as avalanche photodiodes can be used by monitoring leakage through the mirrors. A requirement to ensure identical filtering is that the metrology source light follows exactly the same optical path through the filters as the signal light. Accordingly, the metrology light must be switched into the optical fiber prior to scrambling.

A typical measurement cycle will consist of interleaved atmospheric source and metrology source interferograms, and occasional dark reference cycles. The interleave frequency depends on the CCD readout noise and the expected drift. The metrology source is then used to compensate for drift in the instrument.

Rigid construction of the filter section and interferometer ensures low amplitude component vibrations, on the order of a few pm/√Hz for frequencies above a few Hz in a laboratory environment. Below 1 Hz the noise is dominated by drift and 1/*f* noise. The heaviest contributor to this noise is in the filter section.

Unlike observation of an emission line or a lidar return where a filter is used to reject background light, in an atmospheric absorption measurement the background *is* the signal. For absorption measurements, light must be judiciously rejected at frequencies that do not significantly contribute to a Doppler phase shift. Referring to the instrument diagram in Fig. 3, this condition is accomplished using one or more etalon filters with optimal finesse for the absorption lines of interest. Since the etalon is periodic, a pre-filter is necessary to prevent excess leakage from additional orders. The etalon finesse *F* should be low (*F*~ 6-10), so alignment requirements are somewhat simplified.

By choosing the appropriate free spectral range (FSR), the etalon can be used to filter one absorption line or a pair of lines. There are at least two advantages to filtering an absorption doublet. First, filtering a doublet results in a two-fold increase in the light throughput. Second, using a doublet relaxes the finesse requirement and improves the resolution for etalon tuning.

The spectrum that results from filtering a doublet is illustrated in **Fig. 4**. The complexity of the spectrum forces a precise setting of the interferometer OPD.

The interferometer is a simple Michelson, where one of the mirrors is tilted slightly to produce a spatial fringe pattern on a linear CCD sensor. The interferometer has no moving parts and a fixed-value OPD. A shift in the fringe pattern is a measure of the Doppler shift of an absorption line; however, shifts may occur for numerous other reasons, including filter drift, thermal drift in the interferometer mirrors or simply bending in the housing causing the CCD to physically move. In order to make precision Doppler wind measurements, the interferometer and its associated components must be stable to a few parts in 10^8 over a measurement cycle. **Fig. 5** shows the design for the system, where

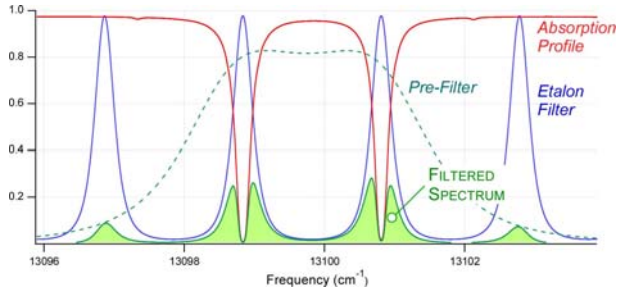

Fig. 4. An absorption line must be optimally filtered to provide a spectrum suitable for wind speed recovery. *Shown here is an example using an etalon filter and a pre-filter to generate a usable spectrum for an interferometer measurement. The absorption profile shifts as the wind speed changes, causing a subtle change in the filtered spectrum.*

the interferometer components are directly bonded to a small Zerodur base. The Zerodur base and all other components, including the CCD sensor, are bonded to a solid low-CTE ceramic, which prevents any significant expansion or bending that would be interpreted as a fringe shift. The interferometer aperture is shared by several independent sources in the form of a linear array of fibers. The outer structure is a fairly thick aluminum frame maintained at a temperature near 23.0 ± 0.1 ºC.

The interferogram obtained with the CCD is analyzed using a proprietary technique that is capable of resolving phase shifts much less than 1 m/sec wind speed equivalent. Accuracy is limited only by the metrology source stability and system drift between calibration cycles. With relatively fast calibration cycles, system drift can be significantly reduced.

The interferometer and the etalon can be considered as a complementary pair in the design. Specifically, air pressure variations in an air-spaced etalon exactly cancel any pressure variations in the air-spaced Michelson. This beneficial result will be irrelevant for a system on orbit, but it is an indication that the same instrument may be used on an aircraft platform at varying altitudes without serious performance degradation. In addition, if the etalon spacer posts are the same material as the interferometer bench, the effect of thermal expansion on the interferogram also is mostly mitigated.

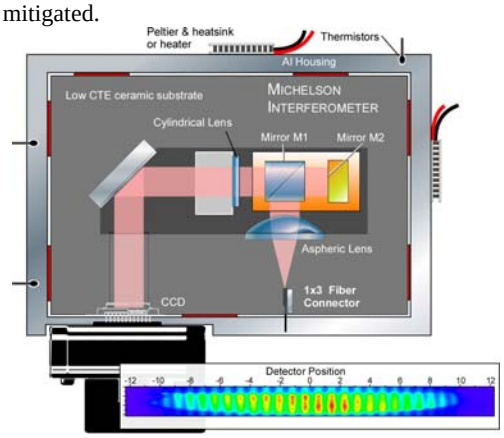

Fig. 5. Schematic view of the interferometer. *All components are permanently bonded to low expansion substrates. The mirror M2 is tilted slightly to produce a spatial interferogram at the plane defined by the CCD array. Several optical fiber sources can share the interferometer aperture and the CCD. There are no moving parts in the structure. An example interferogram taken with the breadboard instrument is shown in the inset.*

The choice of OPD for the interferometer requires careful attention to the intended absorption feature. An example calculation for the fringe visibility and sensitivity is shown in **Fig. 6** as a function of OPD. The function $F(\tau)$ in equation (2) shows up here in the rapidly varying sensitivity curve. In general the best results will occur at peaks of the visibility.

In limb viewing, the absorption lines will have varying width and depth and the filter function should be optimized for viewing at specific column heights. Therefore, several filters likely will be necessary to measure the desired 20-km limb altitude range, but it may be possible for all of the filters to share a single interferometer.

The laboratory measurement approach is represented in **Fig. 7**. To attain repeatable wind speeds, a relatively long "wind tunnel" was constructed for the optical beam to follow. The light source is a communications-grade LED with a room temperature wavelength at 780 nm. Since the instrument is fiber coupled, it is straightforward to include fiber switching components that can alternate the light direction with regard to the air flow. This arrangement enables repeated differential Doppler shift measurements. The interferometer and filter section reside in a vacuum chamber, which will help reduce pressure and temperature fluctuations. Computer control is used for switching in the metrology source for tuning the etalons, taking dark-level background measurements, reading out the CCD, monitoring and controlling temperature, changing the light direction in the wind tunnel, and handing off local feedback control of the etalons during a measurement cycle.

From breadboard measurements and calculations the RMS noise in the engineering unit is expected to approach about 5 m/sec wind speed resolution for 30 second integration times, and perhaps as low as 1 m/sec for measurements that take place in one second or less. The maximum noise contribution likely will come from drifts in the etalon. The theoretical resolution is about 0.1 m/sec at the shot noise limit.

The system throughput is limited primarily by the Michelson interferometer (which represents a 3 dB loss). All other components, including fibers, are expected to add roughly 3 dB of additional loss to the engineering model. With careful design, the throughput loss from telescope focus to CCD can be as low as about 5 dB. Since the finesse of the etalons is low (for optimal absorption line filtering) the etalon throughput mainly will be degraded only by contamination on the mirror surfaces during its lifetime, which is not expected to be significant.

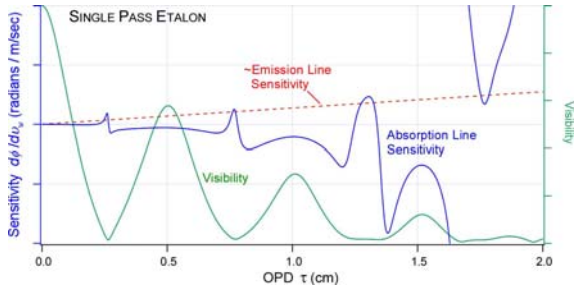

Fig. 6. Representative curves showing the visibility and interferometer sensitivity to wind speed changes as a function of OPD. *The calculations were performed for a 50-m optical path in air, which is consistent with the laboratory experiments. The filter is a single etalon optimized for measuring a relatively shallow oxygen absorption doublet. The dashed curve is the sensitivity expected for an emission line. Note that the sensitivity for the absorption lines has generally the opposite sign in this OPD range.*

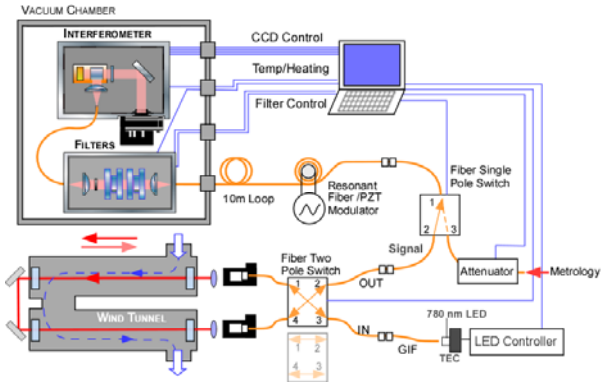

Fig. 7. Schematic of the experimental arrangement for laboratory testing. *The main sub-systems are the interferometer, the filter section, the wind tunnel and computer acquisition and control. To automate the data acquisition, a photonic switching network is included to quickly provide both forward and backward wind directions.*

4. CONCLUSIONS

Since PAWS is targeting measurements low in the atmosphere, Doppler shifts in absorption lines rather than emission lines are used to determine wind speed. The narrow absorption lines are buried in a relatively broad background signal, which complicates the measurement sensitivity (Fig. 6) and imposes a stringent requirement for the stability of the filter. Test results from the breadboard instrument confirmed that the complete system is capable of high-resolution phase measurements and indicated that a metrology source is required for monitoring and maintaining filter position. An engineering unit was designed and is under construction that maximizes stability, signal, and sensitivity within the cost constraints of the project. Measurement of known wind speed in a laboratory wind tunnel will be used to calibrate the system and verify performance. Analysis predicts that the engineering unit will have an equivalent Doppler shift noise level of approximately 5 m/s.

ACKNOWLEDGMENTS

This work was funded through the NASA ESTO Instrument Incubator program, contract number NNG06HX07C. We gratefully acknowledge the support of NASA ESTO, and our COTR, Janice Buckner.

REFERENCES

[1] "Earth science and applications from space: National imperatives for the next decade and beyond." The National Academies Press, Washington, DC, 2007.

[2] G.G. Shepherd, G. Thuillier, W.A. Gault, B.H. Solheim, C. Hersom, J.M. Alunni, J.F. Brun, S. Brune, P. Charlot, L.L. Cogger, D.L. Desaulniers, W.F.J. Evans, R.L. Gattinger, F. Girod, D. Harvie, R.H. Hum, D.J.W. Kendall, E.J. Llewellyn, R.P. Lowe, J. Ohrt, F. Pasternak, O. Peillet, I. Powell, Y. Rochon, W.E. Ward, R.H. Wiens, and J. Wimperis, "WINDII, the wind imaging

interferometer on the Upper Atmosphere Research Satellite," *J. Geophys. Res.*, vol. 98, pp. 10725-10750, June 1993.
[3] P. Rahnama, Y.J. Rochon, I.C. McDade, G.G. Shepherd, W.A. Gault, and A. Scott, "Satellite measurement of stratospheric winds and ozone using Doppler Michelson interferometry. Part I: instrument model and measurement simulation," *J. Atmos. Oceanic Tech.*, vol. 23, pp. 753-769, June 2006.